Check for updates

JOURNAL OF
CELLULAR
PLASTICS

Original article

Journal of Cellular Plastics
2016, Vol. 52(3) 299–319
© The Author(s) 2015
Reprints and permissions:
sagepub.co.uk/journalsPermissions.nav
DOI: 10.1177/0021955X15570077
cel.sagepub.com
SAGE

Injection molded components with functionally graded foam structures – Procedure and essential results

Hans-Peter Heim and Mike Tromm

Abstract

In the past few years, foam injection molding has increasingly gained significance in the field of technical plastic components. This is due to the development of new processes and processing combinations and efforts to produce lightweight products. In this article, a special tool technology will be introduced, which aids the process of expanding the existing areas of applications. The technology enables the production of foam injection molded components with different foaming ratios. This is made possible by core movements in the closed injection mold after the cavity has been filled volumetrically with plastic melt containing blowing agent. In doing so, functionally graded components with locally differing properties can be produced in one processing step. The method (pull and foam method) is based on the idea of equipping thin-walled components with locally foamed thick-volume elements – i.e. to increase the stiffness, create spacers, or joining surfaces. Simultaneously this method aims to exceed the limitations of conventional foam injection molding, especially with regard to scope for design. This article describes the procedure and characteristics of the process. Results with regard to the density in the differentially foamed areas, the morphology and the mechanical properties in correlation with the essential processing parameters are given.

Keywords

Foam injection molding, precision mold opening, breathing mold, pull and foam, local foaming, functional gradation, core pulling, foam density, foam morphology, bending properties

Institute of Materials Engineering – Plastics Technology, University of Kassel, Germany

Corresponding author:
Mike Tromm, Institute of Materials Engineering – Plastics Technology, University of Kassel, Mönchebergstraße 3, D-34125 Kassel, Germany.
Email: tromm@uni-kassel.de

Introduction

The special tool technology is, in principle, a variation or further development of precision mold opening (PMO) which is also referred to as the breathing mold or negative compression process. In the standard PMO method, the cavity is volumetrically filled with melt containing blowing agent. After a short delay time which leads to a further development of compact skin layers, the entire cavity is opened to a predefined extent. Here, mostly molds with shearing edges are used. The pressure drop induced by the sudden increase in volume initiates the foaming process. Opening is mostly realized by a movement of the clamping unit. Generally, the foaming process takes place in the whole component and the result is a component with a compact skin layer and a foamed core area with closed cells. In doing so, a significantly higher degree of foaming, a flow path independent homogeneous distribution of the density and an improved surface quality can be achieved in comparison to conventional foam injection molding.

In contrast to PMO, in the pull and foam method the whole cavity is not extended; instead, only selected areas within the cavity are enlarged. After the mold has been filled volumetrically and the thin-walled areas are frozen, further volume is created by pulling cores inside the closed mold. The thus induced drop in pressure causes the polymer-blowing-agent mixture to expand mainly in these areas. The procedure enables various formations and movement directions of the cores, as well as the possibility to create locally foamed structures while adjacent areas remain nearly compact. The pull and foam method is, in comparison to standard precision mold opening, more flexible, because foaming is not only limited to the mold parting plane. Also, with regard to process control, the pull and foam method is exceptional, because cores are moved inside the closed mold and not by means of opening the clamping unit like in standard PMO.

A unique characteristic of the pull and foam method is the possibility to produce foamed components with extreme differences in wall thickness which cannot be manufactured in this form using other injection molding methods. In the case of conventional foam injection molding, varying wall thicknesses are viewed critically. The high pressure drop at the moment the melt front flows from thin-walled to large cross sections can lead to degassing. Thus, an incomplete filling of the component can occur. As a result, the scope for design of compact and conventionally injection molded, ribbed components can be significantly enlarged. Filling problems in foamed ribs caused by free foaming or the arrangement of the ribs in the flow direction do not occur as they do in conventional foam injection molding, because the ribs are created in the second processing step by means of pulling the core after filling the cavity entirely.

In recent years, some intensive research projects were carried out to describe the correlations between process, foam structure and properties with regard to the conventional PMO process. Kirschling,[1] Bledzki et al.,[2] Flórez Sastre,[3] and Michaeli et al.[4,5] carried out investigations with polycarbonate (PC), while Kirschling and Rohleder involved the gas counter pressure technology. Spörrer,[6–8] Müller,[9,10] and Park et al.[11] did investigations with various

polypropylenes (PP), while Spörrer and Park also involved gas counter pressure and Spörrer additionally considered variothermal mold temperature control. Kühn-Gajdzik[12] focused on PP and PC/acrylonitrile–butadiene-styrene (ABS) inter alia as well under inclusion of gas counter pressure technology.

Regarding the pull and foam process the influence of process control on the structure, the correlating mechanical properties, and the surface quality—in other words the essential processing parameters—are principally the same as those for standard PMO. Structural differences result due to the simultaneous development of neighboring areas with strongly varying degrees of foaming. The experiments have shown, that besides the expanded areas, the thin-walled areas without a cavity enlargement are also influenced by the foaming process. Regarding the demonstrator component, the generally divergent ratios of the foamed core volume in relation to the all-side skin layer—which is constantly in contact with the cooled mold wall—strongly differs when compared to conventional standard PMO geometries. Thus, the area of cooled surface in relation to the heat capacity in the affected melt volume is significantly larger. This leads to a restricted process window and affects the formation of cell structure and the all-side skin layer. The associated conditions strongly influence the structure formation and thus the resulting properties. Mechanical tests have shown that density-specific, higher flexural modulus of elasticity than for the compact material can be achieved up to an expansion ratio of approximately 2, which correlates with a density reduction of approximately 40%. First results have already been published in previous studies; figures for the description of the process and the sample preparation (Figure 1–4) are represented in a similar form.[13–19]

In the following section the process sequence is described and illustrated in Figure 1.

In the first processing step, as is done in conventional PMO, the cavity is volumetrically filled with melt containing blowing agent (1). A high injection pressure or a high injection speed helps to counteract instant foaming. However, because it cannot be avoided completely, an as compact as possible filling of the mold with a minimal degree of foaming is aimed for. An optional short delay time enables a more distinct development of the skin layers and the thin-walled areas; more specifically, areas that should have minimal foaming (2). Pulling cores in the closed mold lead to a local enlargement of the cavity volume. The correlating pressure drop initiates the actual foaming process in the enlarged cavity volume (3). The remaining cooling time and demolding are carried out the same as in a standard injection molding process (4 + 5).

Experimental details

The investigations were carried out using an amorphous and a semi-crystalline material:

- PC/ABS (M/MB5, Schulablend®, Schulmann): $\rho = 1.13\,g/cm^3$, MVR = 14 cm^3/10 min
- PP (RF365MO, Borealis): $\rho = 0.905\,g/cm^3$; MVR = 29 cm^3/10 min

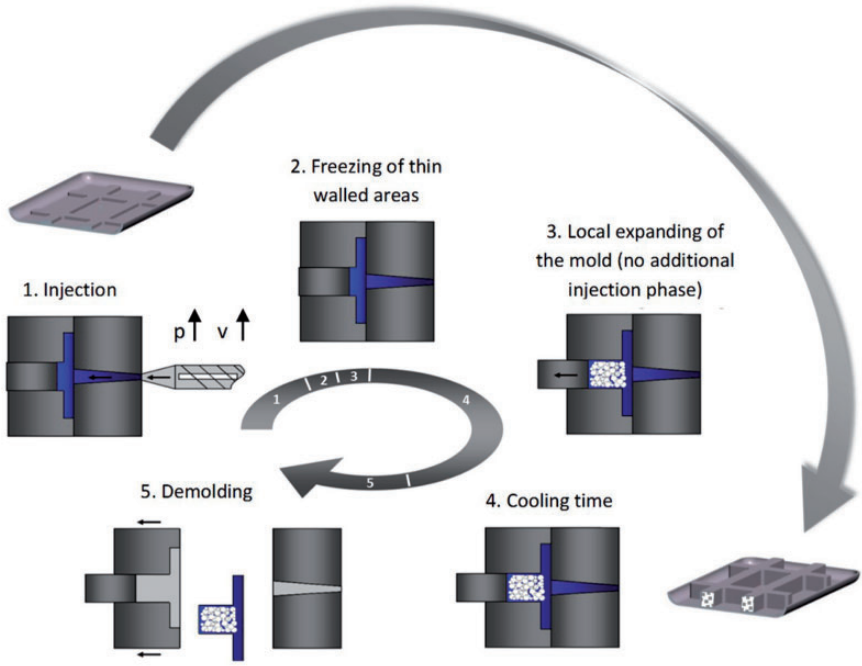

Figure 1. Process sequence of the pull and foam method.[14,15]

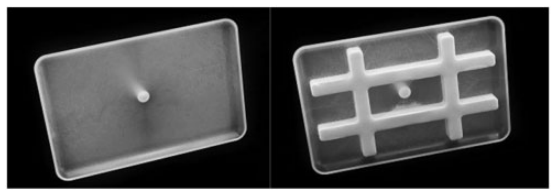

Figure 2. Demonstration component with variable rib height from 0 to 9 mm.[14,15]

The essential processing parameters were identified in pre-tests and the processing windows of the materials were determined. Besides parameters such as injection speed, material temperature and mold temperature, the following process-specific parameters are significant:

- *Blowing agent content (BAC):* The physical blowing agent nitrogen was used for all investigations. It was induced by the MuCell process. The content, meaning the level of supercritical fluid (SCF) in the melt, was varied within the processing window for each material. Here, the gas content was varied between a minimum and maximum recommended value adjusted to the according polymer.

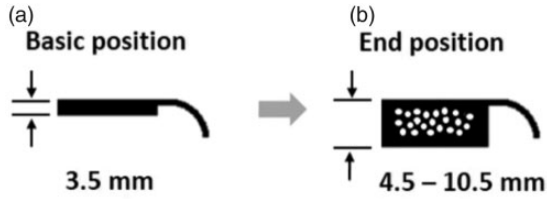

Figure 3. Cross section of the component: (a) component in basic position after volumetrically injecting of material (1st step); (b) component after pulling the core (3rd step).[18]

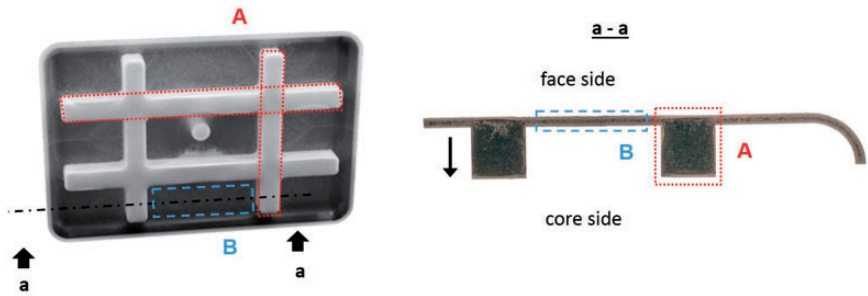

Figure 4. Description of examined areas of the demonstrator component.[18]

- *Expansion ratio (ER):* This parameter indicates the volume expansion. It is defined as volume of the rib area after pulling the core in relation to its basic volume. The parameter can directly be set by the adjustable core of the demonstrator mold.
- *Delay time (t_D):* This parameter is defined as the time between end of volumetrically injection phase (EOF) and pulling the core. Compared with similar investigations with standard PMO, the delay time could only be varied in a restricted range. The expandable geometry of the demonstrator component exhibits a lower ratio of volume in relation to its surface than conventional PMO components. The surface which is in contact to the cooled mold wall is thus significantly higher. This leads to a more rapid cooling of the melt and, consequently, to a more restricted process window—concerning the delay time. A high delay time in combination with a high expansion ratio leads to insufficient molding or sink marks at the surface of the component.

Based on material-specific, robust processing settings, these process-specific parameters were varied so as to be able to assess how the structure and properties are influenced. In Table 1, the fundamental processing conditions and the variation of the process-specific parameters are displayed.

Components with different process settings were produced using a demonstrator mold. The geometry of the demonstrator component is a thin-walled plate with the

Table 1. Processing parameters.

	PC/ABS	PP
Melt temperature (°C)	265	230
Mold / Core[a] temperature (°C)	75	75
Injection speed (mm/s)	40	35
Cooling time (s)	20	25
Back pressure (bar)	120	140
Core speed (mm/s)[b]	approx. 50	approx. 50
Expansion ratio *ER* (–)	1.29/1.57/2.14/2.71	1.29/1.57/2.14/2.71/3
Blowing agent content *SCF* (wt%)	0.4/0.8	0.5/1.0
Delay time t_D (s)	0/1	0/1

[a]The temperature of the core was not maintained separately.
[b]Measurement carried out in open mold.

dimensions 120 mm × 80 mm and a wall thickness of 1.5 mm. A movable core insert in form of a crossed ribbed construction enables an enlargement of the volume of the cavity. Thus, 8 mm wide ribs with a continuous, adjustable height of 0–9 mm can be molded on the backside of the plate (see Figure 2).

A basic position with a rib height of 2 mm was set for all tests (additional 1.5 mm component wall thickness → total thickness of rib = 3.5 mm). In this basic position (Figure 3(a)), the mold was filled volumetrically with melt containing blowing agent. No holding pressure was applied. Even if delay time was set also no holding pressure was applied for this time. Afterwards, the crossed ribbed section was pulled up to different end positions. A maximum position of 9 mm was realized—additional 1.5 mm component wall thickness → total thickness of rib = 10.5 mm (see Figure 3(b)). In consideration of the total thickness, this is equivalent to an expansion ratio of maximally 3.0 ($ER = 10.5\,\text{mm}/3.5\,\text{mm}$). The core itself is moved by a hydraulic cylinder. The speed of the core movement can only be adjusted in a small restricted range by controlling the oil pressure. Thus, it was kept constant for all materials and process settings. Due to the correlating pressure drop that takes place in this area, the essential part of foaming takes place here.

The areas A and B highlighted in Figure 4, were cut out of the components and used for density measurements and the investigations on the morphology. In order to characterize the mechanical properties, three-point bending tests were carried out for the foamed areas (Figure 4 – area A).

Results

Morphology

There are basic differences in the formation of the morphology by foaming amorphous and semi-crystalline materials. Generally, amorphous polymers show

a wider processing window and more homogeneous cell structures. Here, in general only homogeneous nucleation takes place. Using semi-crystalline polymers it is harder to control the foaming process. Crystals act as heterogeneous nucleation cites. Crystallization affects the rheology and thus the foaming process. The interactions are complex. They normally show a narrow process window. The solubility and the formation of pores depends, among others, on the crystallinity of the material. By increasing crystallinity the solubility of gases diminishes. Diffusion and absorption processes take place in the amorphous regions. Solubility and pore density decrease by increasing crystallinity. Thus, materials with less crystallinity can uptake more gas. This leads to higher thermodynamic instability, thus to an increase in pore density and a more homogeneous structure. Furthermore, semi-crystalline polymers exhibit a faster freezing of the melt front. Hereby, as a tendency, thinner compact skin layers are created.[12,20,21]

In the following, the morphology of the two different materials used in this investigation are described. The specimens were embedded in resin, grinded, and polished. The pictures were taken with a digital light microscope (Keyence VHX 600). The skin layer thicknesses and pore sizes were investigated using photo editing software. For the skin layer thickness, large areas were selected and the mean skin layer thicknesses were calculated.

PC/ABS exhibits a distinct fine-celled pore structure with a pore diameter in the center of the component between 30 µm and 70 µm (median). A clearly separated compact skin layer can be observed at all process settings. The pores exhibit a high roundness and an alignment of the pores cannot be observed. An increasing expansion ratio leads to an increase in pore diameter and pore size distribution (see Figure 5). An increase in delay time also leads to a coarse structure (see Figure 6). In combination with a high expansion ratio incomplete molded components can occur. In extreme cases, sink marks at the visible side of the component or a fracturing of the flanks of the ribs occur (see Figure 7). It is assumed that in the case of high delay times the melt is too cold at the moment the core is pulled.

An increase in the blowing agent content does not seem to affect the structure in a great extent (see Figure 8).

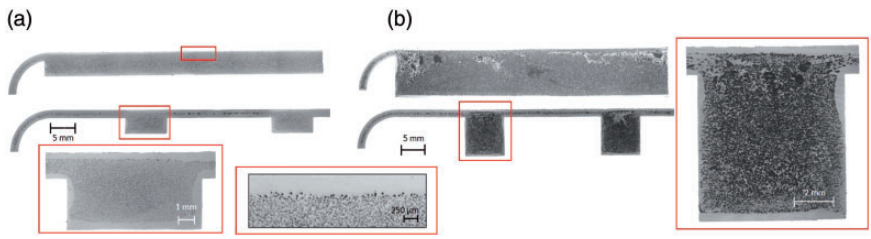

Figure 5. Morphology of physically foamed PC/ABS ($SCF = 0.4$ wt%, $t_D = 0$ s) at different expansion ratios: (a) $ER = 1.29$; (b) $ER = 2.71$.

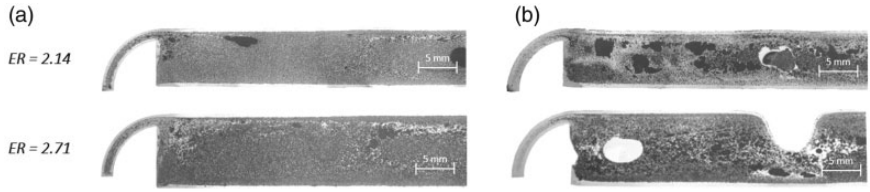

Figure 6. Morphology of physically foamed PC/ABS at two different expansion ratios ($ER = 2.14$ and 2.71) at different delay times: (a) $t_D = 0$ s; (b) $t_D = 1$ s.

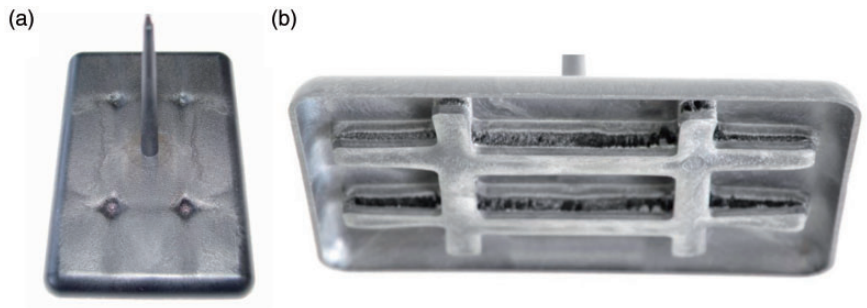

Figure 7. Component of PC/ABS – combination of high expansion ratio and high delay time ($ER = 3$, $t_D = 1$ s, $SCF = 0.8$ wt%): (a) sink marks on face side above back-facing ribs; (b) fracturing of rib flanks.

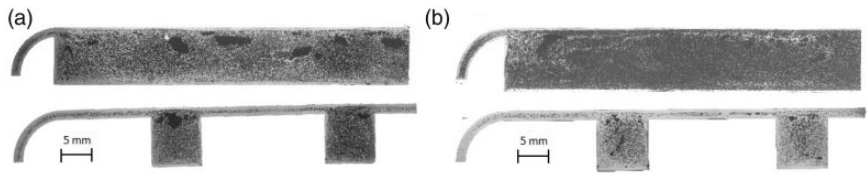

Figure 8. Morphology of physically foamed PC/ABS ($ER = 2.71$, $t_D = 0$ s) at two different blowing agent contents: (a) $SCF = 0.4$ wt%; (b) $SCF = 0.8$ wt%.

Table 2 gives an overview of the skin and core layer thicknesses for PC/ABS.

The compact skin layer thickness on the face side as well as on the core side decreases with an increasing expansion ratio. A slight decrease can also be investigated for higher blowing agent contents. Similar effects are described by Kirschling[1] and in previous studies.[18] Expectedly, a delay time of 1 s—which correlates with a higher amount of heat conduction to the mold wall—leads to an increase in skin layer thickness.

In contrast to PC/ABS, PP shows a coarse, inhomogeneous structure with a mean pore diameter in the center of the sample of 190–700 μm (median). The pores are partly shaped in direction of the core movement. A clearly defined compact

Table 2. Thickness of skin layers and core layer – PC/ABS

ER (–)	*SFC* (%)	t_D (s)	Skin layer face side (%)	Skin layer core side (%)	Core layer (%)
1.29	0.4	0	11.26	12.16	76.59
	0.8	0	10.49	11.68	77.83
	0.8	1	12.87	12.97	74.17
1.57	0.4	0	8.48	9.18	82.35
	0.8	0	8.16	9.17	82.68
	0.8	1	8.16	9.5	82.34
2.14	0.4	0	5.57	5.48	88.95
	0.8	0	4,94	6.06	89.01
	0.8	1	5.71	7.03	87.26
2.71	0.4	0	5.17	5.62	89.22
	0.8	0	3.6	4.14	92.26
	0.8	1	4.05	6.11	89.83

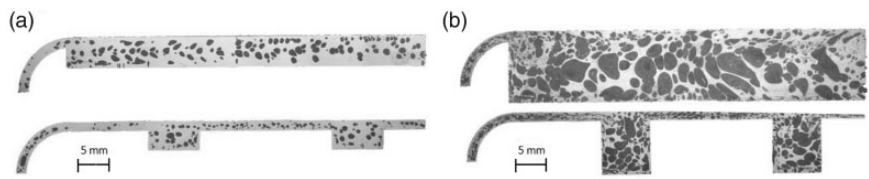

Figure 9. Morphology of physically foamed PP (*SCF* = 0.5 wt%, t_D = 0 s) at different expansion ratios: (a) *ER* = 1.29; (b) *ER* = 2.71.

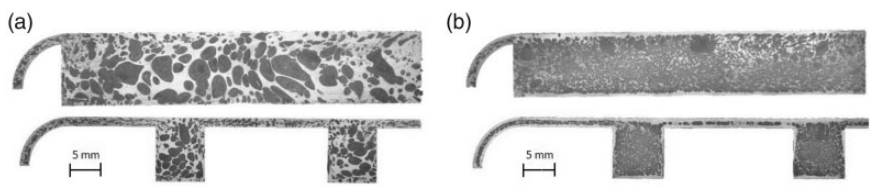

Figure 10. Morphology of physically foamed PP (*ER* = 2.71, t_D = 0 s) at different blowing agent contents: (a) *SCF* = 0.5 wt%; (b) *SCF* = 1.0 wt%.

skin layer, as expected in foam injection molding, can only be observed partly. By analogy of PC/ABS, with an increasing expansion ratio the pore diameter and the pore size distribution increase. The pores are strongly deformed and coalesced (see Figure 9). Process settings with low blowing agent content (see Figure 10) or high delay times (see Figure 11) also lead to a coarse, inhomogeneous structure with big pores which partly reach the component's surface. Here, the compact skin layer is partly interrupted. Particularly, the combination of low blowing agent content,

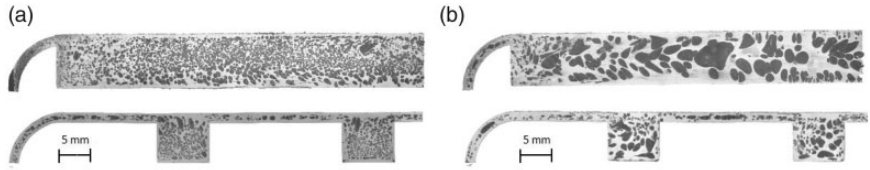

Figure 11. Morphology of physically foamed PP ($ER = 2.14$, $SCF = 0.5$ wt%) at different delay times: (a) $t_D = 0$ s; (b) $t_D = 1$ s.

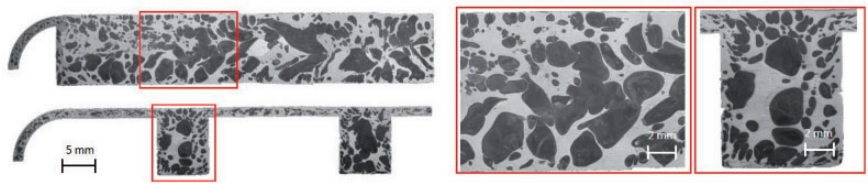

Figure 12. Morphology of physically foamed PP ($ER = 2.71$, $SCF = 0.5$ wt%, $t_D = 1$ s)—combination of high expansion ratio, low blowing agent content, and high delay time

Table 3. Thickness of skin layers and core layer – PP.

ER (–)	*SFC* (%)	t_D (s)	Skin layer face side (%)	Skin layer core side (%)	Core layer (%)
1.29	0.5	0	N/A	N/A	N/A
	0.5	1	20.62	27.37	52.01
1.57	0,5	0	14.13	13.05	72.83
	1.0	0	10.01	13.36	76.63
2.14	0.5	0	8.27	N/A	N/A
	0.5	1	10.68	10.04	79.28
2.71	0.5	0	N/A	N/A	N/A
	1.0	0	5.64	5.38	88.98
3.00	0.5	0	N/A	N/A	N/A
	0.5	1	N/A	N/A	N/A

N/A: no data evaluable because of the inhomogeneous structures.

high expansion ratio, and high delay time leads to structures where no compact skin layer can be identified (see Figure 12). The variation of blowing agent content—in the range of these investigations—shows a dominant effect on the structure.

Table 3 gives an overview of the skin and core layer thicknesses for PP. As can be seen in the last figures, for some process settings no representative data could be evaluated.

As well for PP, the compact skin layer thickness decreases with an increasing expansion ratio, as also described by Müller.[10] The influence of blowing agent content and delay time cannot quantifiable be assessed because of the inhomogeneous structures.

To quantify the pore sizes, a homogeneous section in the center of the specimen was selected. Single pore areas were measured and the average pore diameter or pore median was calculated. A homogeneous area without defects in the center of the foamed structure was selected. The areas of the pores were measured at a magnification of 200 × (PP) and 500 × (PC/ABS) by the help of photo-editing software. Thus, the pore diameter was calculated. Using this method, exact absolute values cannot be determined. On the one hand, the idealization is made, that pores are ideal-round shaped. On the other hand, a measurement error occurs because in this two-dimensional cut the pores are cut in their center in the rarest cases. Thus, mostly off-center cut areas were measured. This effect is described as the tomato slice effect in literature. Due to the fact, a slightly lower pore diameter than in reality was calculated. However, this measurement error is of a systematic nature and does not affect the estimation of the qualitative influence. To obtain statistical certainty, three components of each test setting, thus up to 1000 values per test setting were measured. Due to the high number of results, an assessment in form of box plots is recommendable (Figures 13 and 14). It enables a large number of measurement values to be displayed clearly. The distribution and scattering of the different process settings can

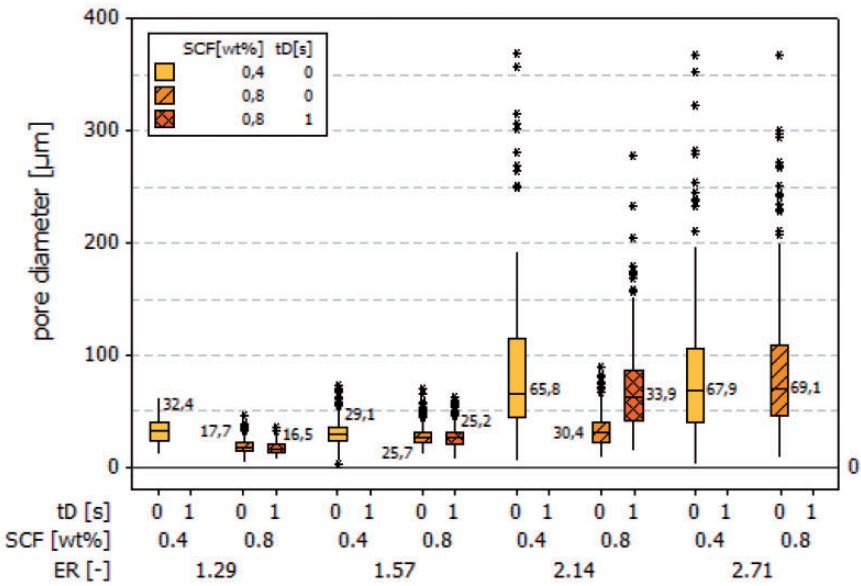

Figure 13. Calculated pore diameter of physically foamed PC/ABS at different process settings.
tD: delay time; SCF: supercritical fluid; ER: expansion ratio. (Figure based on Heim and Tromm[18] – additional data was added).

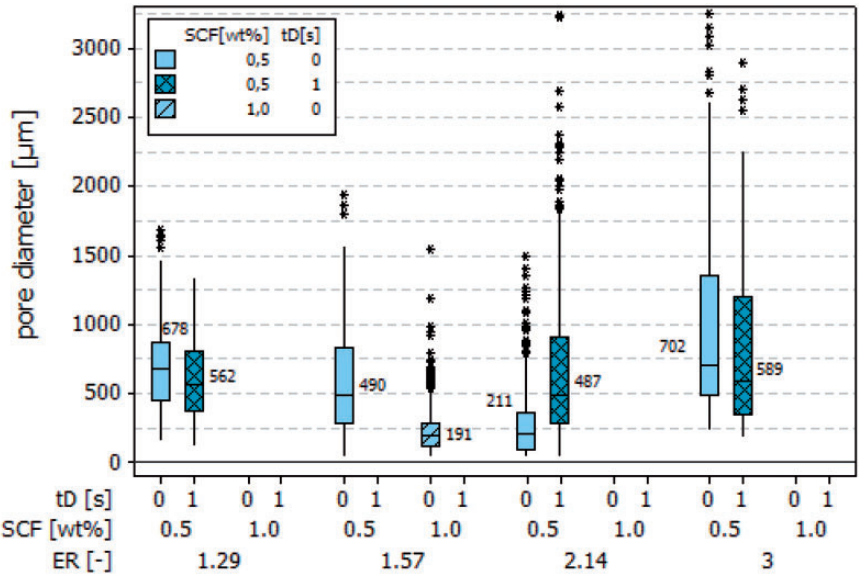

Figure 14. Calculated pore diameter of physically foamed PP at different process settings. tD: delay time; SCF: supercritical fluid; ER: expansion ratio.

be compared directly. One box represents 50% of the measurement values, and the vertical lines indicate the minimum and maximum deviations. Stars indicate statistical calculated outliers. The horizontal line within each box displays the median value. The median is used, because it is less sensitive against outliers than the arithmetic average. In order to assess the effects of the process parameter settings, both the median and the scattering were considered. Because of the high number of measurements in the following diagrams the number of outliers (stars) seems to be very high. However, the rate of outliers is below 6% in all cases.

The values for PP show a very large scattering and many outliers. But, the data confirms the overall trend, seen in the microscopic pictures. The observed tendency of the pore diameter and the scattering to increase in correlation with an increasing expansion ratio can be confirmed, independently of the material. Comparable results were found by Gómez-Gómez et al.[20] The influence of the delay time on the pore diameter only conditional statements can be made. For PC/ABS no influence can be assessed for low expansion ratios. At an expansion ratio of 2.14 a higher delay time leads to an increase in pore diameter. At higher expansion ratios, the structure is that inhomogeneous that no representative areas for measuring can be selected, thus no data could be determined, as also described in prior studies.[18] For PP, no definite tendency can be observed. But, here only measurement data for low blowing agent content is available. For some process settings, no representative areas could be selected because of the inhomogeneous structures. An increase in blowing agent content leads to smaller pore diameters and lower scattering of data, meaning to a more homogeneous fine-celled structure. More pores are growing simultaneously, thus

there is less space to grow. Similar effects in regard to the influence of the blowing agent were found by Kirschling[1], Kühn-Gajdzik[12] and Gómez-Gómez et al.[20]

Density

Using the Archimedes principle according to DIN EN 1183, density measurements were carried out for the two areas pointed out in Figure 4. Area A is the foamed rib area with a varying expansion ratio and area B is the thin-walled area without cavity enlargement. The expansion ratio and the correlating local density in area A can be directly set by means of the core pulling distance. In area B, the foaming and density cannot be directly influenced and is dependent upon the density in area A, as well as on the processing parameters. Figures 15 and 16 show scatter plots of the relative density values at different densities and process settings. The mean values of each parameter setting are connected by regression lines. The figures illustrate the density of the different areas of the foamed components with regard to the density of the unfoamed, compact parts. The values are plotted as a dimensionless ratio π_ρ (–), defined as density of foam referred to the density of compact material

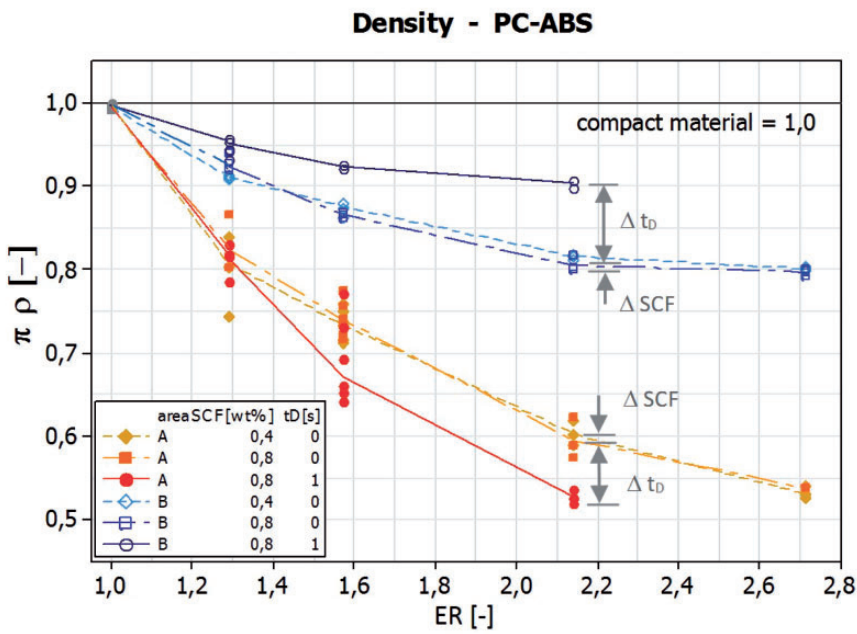

Figure 15. Density in the different areas of the demonstrator component in dependency of the process parameters—PC/ABS.
tD: delay time; SCF: supercritical fluid; ER: expansion ratio. (Figure based on Heim and Tromm[18] – additional data was added).

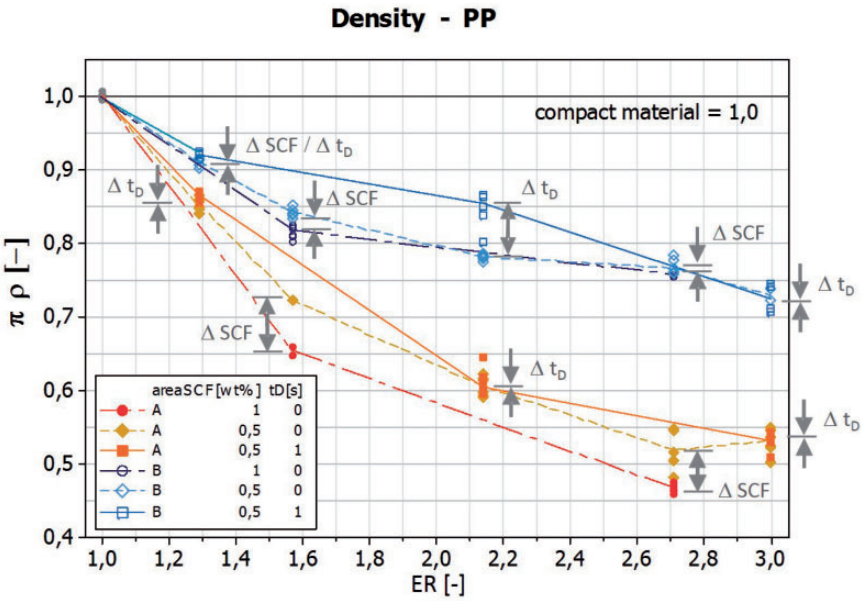

Figure 16. Density in the different areas of the demonstrator component in dependency of the process parameters—PP.
tD: delay time; SCF: supercritical fluid; ER: expansion ratio. (Figure based on Heim and Tromm[19] – additional data was added).

(ρ_{foam} / $\rho_{compact\ material}$), in dependency of the expansion ratio *ER* (–)(final position foamed rib / basic position compact rib). The figure shows two different groups of measurement values, namely the values for the specific foamed area A and for the thin-walled area B at different process settings.

When comparing the materials, some general, process-specific effects can be seen. As expected, an increasing expansion ratio leads to a decrease in density in the foamed rib area (A). At the maximum expansion ratio, a density reduction of approximately 50% results for both investigated materials. However, the density of the thin-walled areas (B) is also affected by the expansion ratio. The higher the expansion ratio and thus the volume of the foamed rib area (A), simultaneously the higher the foaming is in the adjacent, thin-walled area (B). The pressure drop induced by the local enlargement of the cavity also affects the plastic core of the thin-walled area (B). The density reductions at a maximum expansion ratio of 2.71 (PC/ABS) or 3 (PP) in this area are approximately 20–30%. Because of this interaction of both areas, the density reduction in the foamed ribs (A) is not proportional to the expansion ratio.

Regarding PC/ABS, as expected, a high delay time leads to a lower degree of foaming and thus to a higher density in the thin-walled area (B). The longer the delay time, the less melted material is in the thin-walled area (B) at the time the core is pulled. In the area of the foamed ribs (A), the opposite effect is observed.

A longer delay time results in a higher degree of foaming and thus in a lower density. These effects increase in both areas in correlation with an increasing expansion ratio. The effect which could be evaluated for area A is confusing. A longer delay time is accompanied with a longer cooling time, thicker skin layers and a cooler melt. Consequently, a lower foaming degree or higher density should be the result. The explanation here can be the interaction of the two adjacent areas. The delay time was varied ceteris paribus, meaning mass and volume of the component were constant. Hence, a higher density in one area, here in the thin-walled areas, correlates with a lower density in the other area, here in the highly foamed areas. This effect can be seen very clearly for PC/ABS.

Regarding similar process settings for PP in the area of the foamed ribs (A), no effect caused by the delay time can be identified. No definite tendency is observed for PP in the thin-walled area (B). At a medium expansion ratio a lower degree of foaming, resulting in a slightly higher density can be evaluated. For low and high expansion ratios, no difference is discernible after having varied the delay time. It is important to note that the available measurement data of PP refer to a process setting with a low amount of blowing agent content. The results for PP are also described in previous invesigations.[19] The microscopic investigations have shown that in comparison with PC/ABS the formation of the compact skin layer of this process setting of PP is not that clear and continuous and is partly interrupted by pores. Furthermore, the morphology of PP is considerably inhomogeneous in comparison with PC/ABS. Maybe these effects lead to an inhomogeneous density distribution in the component, even in the different areas and as consequence result in indistinct results.

The content of blowing agent proves to have no significant influence in the varied processing windows shown here for PC/ABS, both in the area of the foamed ribs (A) and the thin-walled area (B). The deviations are within the range of measurement scattering. Regarding PP in the area of the foamed ribs (A), it is seen that higher the content of blowing agent, higher the degree of foaming and lower the density. The size of the effect is independent of the expansion ratio. The microscopic investigations have shown that the blowing agent content has a major influence on the morphology for this material and thus also on the density. In the thin-walled area (B), the effect cannot be assessed clearly. The effect has not yet been finally clarified. Further investigations have to be made.

Mechanical properties – Bending test

The scope of application for the special technology described here, is mainly seen in a function of locally stiffening of plane geometries or thin-walled components. Concerning this, especially the bending stiffness is of high significance. The skin layer formation is very important for this testing method. On applying a bending load, the highest stresses occur in the skin areas. Thus, density-specific, foam injection molded components can achieve higher flexural modulus of elasticity than compact material. Because of the special mold technology used, furthermore the skin layer formation in the flanks of the ribs can affect the mechanical properties.

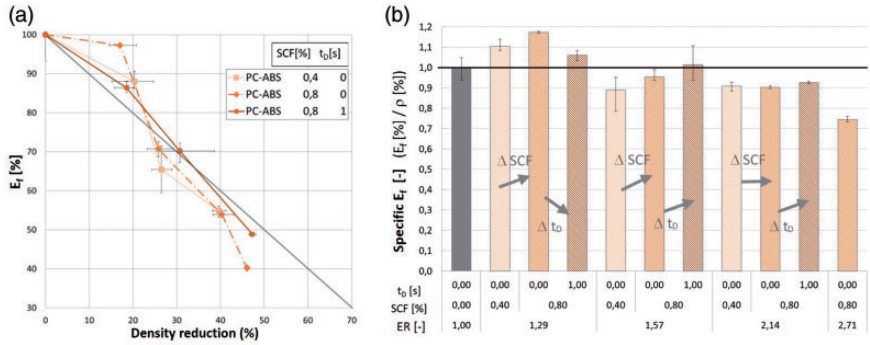

Figure 17. (a) Flexural modulus of elasticity in correlation with the reduction of density; (b) specific flexural modulus of elasticity in correlation with the process parameters – PC/ABS. tD: delay time; SCF: supercritical fluid; ER: expansion ratio.

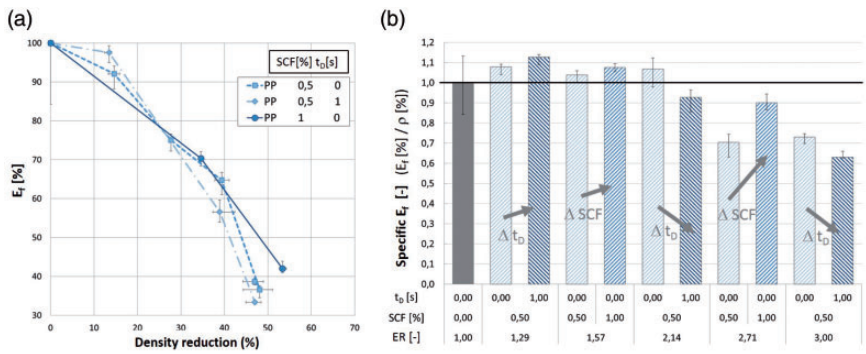

Figure 18. (a) Flexural modulus of elasticity in correlation with the reduction of density; (b) specific flexural modulus of elasticity in correlation with the process parameters – PP. tD: delay time; SCF: supercritical fluid; ER: expansion ratio. (Figures 18 b) based on Heim and Tromm[19] – additional data was added).

In order to determine the mechanical properties, more precisely the bending properties, three-point bending tests according to DIN EN ISO 178 were carried out for the entire components and on cut-free rib areas (area A). The following illustrations (Figures 17 and 18) refer to the cut-free rib areas. The flexural modulus of elasticity E_f in percentage—according to the compact material—is plotted over the density reduction. Every process setting leads to different density formations. Thus, the modulus cannot be compared directly one with another. In order to be able to evaluate the influence of the processing parameters on the mechanical properties, the flexural modulus of elasticity is displayed as a specific, density-related value (E_f (%) / ρ (%)). This specific flexural modulus of elasticity is plotted in correlation with the processing settings. In the illustrations, the decrease in values can be assessed with regard to the density reduction (Figures 17(a) and 18(a)), and with regard to the

influence of the process settings expansion ratio (ER), blowing agent content (SCF), and delay time (t_D) (Figures 17(b) and 18(b)). The error indicators respectively denote the minimum and maximum measurement values.

The flexural modulus of elasticity decreases as the density decreases (Figures 17(a) and 18 a)). Disproportionate value drops can be determined for PC/ABS up to an expansion ratio of 1.29 (density reduction approximately 20%), for PP (low SCF) up to an expansion ratio of 2.14 (density reduction approximately 40%). Up to this expansion ratio, density-specific, higher flexural modulus of elasticity can be achieved than for compact material. However, a disproportionate decline of the modulus values can be identified for higher expansion ratios, meaning the density-specific flexural modulus of elasticity is lower than that of the compact material. As could be seen in the chapter morphology, in general high expansion ratios lead to inhomogeneous structures with larger pores. The pores get bigger and deformed. An increase in pore conclusions and partly larger hollow spaces can be determined. Furthermore, a decrease of the compact skin layer can be determined for increasing expansion ratios. These effects can lead to the decrease in the modulus of elasticity, as also described in previous investigations.[19]

The influence of process control is dependent on the material in the context of the processing windows varied here. On the basis of the density-specific values (Figures 17(b) and 18(b)), a general increase in the modulus and a lower deviation of data can be achieved for PC/ABS and PP with increasing blowing agent content. A high blowing agent content leads to a more homogeneous pore structure. A higher amount of pores, smaller pores and for PP a continuous skin layer is created. Furthermore, as already mentioned in the morphological results, a too low content of blowing agent can lead to very large pores and a noncontinuous skin layer.

For the delay time a uniform trend for the materials cannot be determined, and the influence depends on the expansion ratio and displays opposite directions of effect for PP and PC/ABS. For PP, a long delay time in combination with a low expansion ratio leads to an increase in the specific flexural modulus; in contrast, a high expansion ratio results in a decrease, as also described in prior studies.[19] PC/ABS displays an opposite effect, a long delay time in combination with a low expansion ratio results in low specific flexural modulus, at high expansion ratios a long delay time leads to an increase in the values.

A higher delay time corresponds with a longer cooling time. It is expected that a higher delay time leads to an increase in the compact skin layer thickness, thus to a higher flexural modulus. Similar investigations with conventional PMO have shown this effect.[5,6,7,10] But, the delay time was varied to a larger extend than the restricted variation done in the present study. For PC/ABS the skin layer thickness only slightly increased—approximately 2% of total thickness—at the maximum delay time of 1 s. But regarding the morphological structure for this process setting, often a very fine-celled structure with some big hollow spaces could be evaluated. This could be the reason for the decrease at a process setting of low expansion ratios in combination with a high delay time. The reason for the

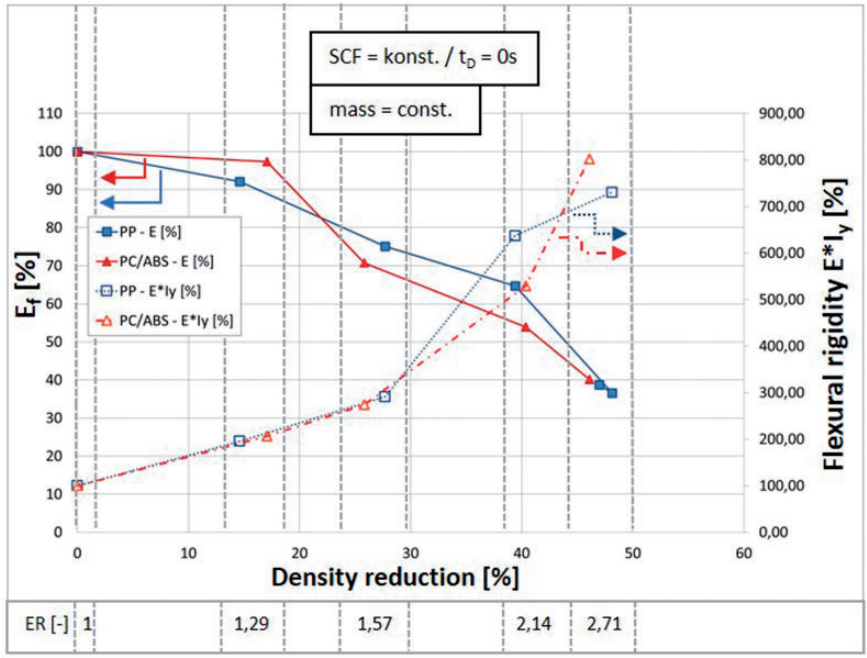

Figure 19. Flexural modulus of elasticity and flexural rigidity in correlation with the density reduction and expansion ratio.
tD: delay time; SCF: supercritical fluid; ER: expansion ratio.

development of these hollow spaces is not clarified yet. For PP, just insufficient data for the skin layer thickness could be evaluated. The reason being the nonuniform skin layer thickness that is partly interrupted by pores. The effect of an increasing inhomogeneity of the structure further increases in combination with a higher delay time. Hereby, the skin layer formation is also affected. It is assumed that these effects counteract the actual influence of the delay time. They seem to have a larger influence on both, structure formation and skin layer thickness, than the longer cooling time which corresponds with a higher delay time.

In general, foaming methods make it possible to achieve higher component stiffness by using the same amount of material due enlarging the component geometry. The flexural modulus does decline by foaming; however, the correlating decrease in stiffness can be overcompensated by the accompany increase in the moment of inertia resulting by the enlargement of the volume. As a result foam injection molding and especially the PMO method, which enables significantly higher expansion ratios, leads to a tremendous potential for lightweight constructions.[8,10,22]

In order to illustrate the potential of foaming in terms of the component stiffness, the measured flexural modulus of elasticity and the calculated flexural rigidity

dependent on the density reduction, which is achieved by an enlargement of the volume, are shown in Figure 19. One process setting is shown per material. The flexural rigidity is a product of the flexural modulus of elasticity (material resistance) and the moment of inertia (geometrically induced resistance). While the flexural modulus of elasticity decreases as the density reduction increases, the moment of inertia increases disproportionately due to the enlargement of the volume. Ultimately, this leads to an increase in the flexural rigidity at a constant component weight, as also depicted in various studies.[8,10,22]

Conclusion

The pull and foam process was investigated by using PP and a PC/ABS blend. The experiments reveal the potential and limitations of this method in terms of structure formation, density reduction, and mechanical properties. The local volume expansion and the geometry of the core lead to differences in processing and results compared with conventional precision mold opening:

1. Effects on structure formation and process window

The height/width ratio of the foamed areas changes during cavity enlargement. Thus, the surface/volume ratio also changes, which is nearly insignificant in conventional precision mold opening. Accordingly, during and after cavity enlargement the area of cooled surface in relation to the heat capacity in the affected melt volume is significantly larger. This leads to a restricted process window and affects the formation of cell structure and skin layer. An excessive variation of the process window leads to inhomogeneous structures and deficient skin layer formation. Pores can be developed up to the component's surface and interrupt the compact skin layer.

2. Effects on density formation

Besides the specifically foamed areas, the thin-walled areas without a cavity enlargement are also influenced by the foaming process. Depending on the material and process settings, density reductions of up to approximately 50% are achieved in the extended areas. In correlation with this, simultaneously density reductions of 20–30 % result in the neighboring, thin-walled areas without a later cavity enlargement.

3. Effects on mechanical properties

The stiffness of components can be improved locally. Depending on the material and the process control, density-specific, higher flexural modulus of elasticity than for the compact material can be achieved up to an expansion ratio of approximately 2 which correlates with a density reduction of approximately 40%. In combination with the volume enhancement, a big potential for lightweight

constructions is achievable. The above mentioned inhomogeneous structures corresponding to an extensive variation of the process window lead to a decrease in the mechanical properties. The results which do not fit the trend correlate with these parameter settings.

Acknowledgement

The authors would like to acknowledge Engel Austria GmbH (Schwertberg, Austria) for working with their injection molding machines in their technical center.

Declaration of Conflicting Interests

The author(s) declared no potential conflicts of interest with respect to the research, authorship, and/or publication of this article.

Funding

The author(s) received no financial support for the research, authorship, and/or publication of this article.

References

1. Kirschling H. *Mikroschäume aus Polycarbonat / Microcellular foams of polycarbonate*. PhD Thesis, University of Kassel, Germany, 2009.
2. Bledzki AK, Rohleder M, Kirschling H, et al. Correlation between morphology and notched impact strength of microcellular foamed polycarbonate. *J Cell Plast* 2010; 46: 415–440.
3. Flórez Sastre L. *Influence of the foam morphology on the mechanical properties of structural foams*. PhD Thesis, University of Aachen, Germany, 2011.
4. Michaeli W, Flórez L and Oberloer D. Schaumdesign / Foam design. *Plastverarbeiter* 2009; 4: 80–82.
5. Michaeli W, Florez L, Oberloer D, et al. Analysis of the impact properties of structural foams. *J Cell Plast* 2009; 45: 321.
6. Spörrer A. *Leichte Integralschaumstrukturen durch Spritzgießen mit optimierten Werkstoffen und variothermen Werkzeugen / Lightweight structural foams by injection molding with optimized materials and variotherm tools*. PhD Thesis, University of Bayreuth, Germany, 2010.
7. Spörrer A. The challenge of foam injection moulding – possibilities to improve surface appearance, foam morphology and mechanical properties. In: *Blowing agents and foaming processes 2007 (Smithers Rapra)*, Frankfurt (Main), Germany, 22–23 May 2007, paper no 16.
8. Spörrer A and Altstädt V. Controlling morphology of injection molded structural foams by mold design and processing parameters. *J Cell Plast* 2007; 43: 313.
9. Müller N and Ehrenstein GW. Evaluation and modeling of injection-molded rigid polypropylene integral foam. *J Cell Plast* 2004; 40: 45.
10. Müller N. *Spritzgegossene Integralschaumstrukturen mit ausgeprägter Dichtereduktion / Injection molded integral foams with pronounced density-reduction*. PhD Thesis, University of Erlangen-Nuremberg, Germany, 2006.

11. Lee JWS, Wang J, Kim SG, et al. Advanced structural foam molding of various PPs with gas counterpressure and mold opening. In: *Polymer foam 2007 (AMI)*, Newark, NJ, USA, 2–3 October 2007, pp. 1–14.
12. Kühn-Gajdzik J. *Amorphe und teilkristalline Mikroschäume im Spritzgießverfahren / Amorphous and semi-crystalline microcellular foams by injection molding*. PhD Thesis, University of Kassel, Germany, 2011.
13. Heim H-P, Schnieders J, Jarka S, et al. Geschäumte Rippen für dünnwandige Teile / Foamed ribs for thin-walled components. *Kunststoffe* 2011; 9: 48–50.
14. Heim H-P, Tromm M, Jarka S, et al. Pull and foam - Injection moulding method: Foamed ribs for stiffening plane components. In: *ANTEC (SPE)*, Orlando, FL, USA, 2–4 April 2012, pp. 2477–2480.
15. Heim H-P and Tromm M. Pull and foam – method: First investigations with chemical and physical blowing agents. In: *10th International conference on foam materials & technology, FOAMS (SPE)*, Barcelona, Spain, 12–13 September 2012.
16. Heim H-P, Bledzki AK, Rohleder M, et al. Thermo-mechanically graded injection moulded microcellular foams. In: *1st International conference on thermo-mechanically graded materials*, Kassel, Germany, 29–30 October 2012, pp. 231–240.
17. Heim H-P, Beldzki AK, Rohleder M, et al. Formation of foam structures and influence of processing procedure in foam injection moulding of thermoplastic materials. In: *2nd International conference on cellular materials*, Dresden, Germany, 7–9 November 2012.
18. Heim H-P and Tromm M. Formation of morphology as a function of process control by foam injection molding of a functionally graded components. In: *ANTEC (SPE)*, Las Vegas, NV, USA, 28–30 April 2014, pp. 1551–1556.
19. Heim H-P and Tromm M. General aspects of foam injection molding using local precision mold opening technology. *Polymer* 2015; 56: 111–118.
20. Gómez-Gómez FJ, Arencón D, Sánchez-Soto MÁ, et al. Influence of the injection moulding parameters on the microstructure and thermal properties of microcellular polyethylene terephthalate glycol foams. *J Cell Plast* 2013; 49(1): 47–63.
21. Liao R, Yu W and Zhou C. Rheological control in foaming polymeric materials: II. Semi-crystalline polymers. *Polymer* 2010; 51: 6334–6345.
22. Roch A, Menrath A and Huber T. Fiber reinforced thermoplastics in sandwich construction. *Kunststoffe Int* 2013; 10: 119–124.